Engineering Perspectives in Filtration and Separation, Vol. 3, No. 1, 2025
ISSN:3107-5290

Energy-Efficient Microalgae Filtering and Harvesting Using an Extremely Low-Pressure Membrane Filter with Fouling Control

Dr. Elena Petrova[1] and Dr. David Kowalski[2]*

[1]Senior Researcher, Environmental Science and Chemical Engineering, Moscow State University, Russia.*

[2]Professor, Environmental Science and Chemical Engineering, Moscow State University, Russia.

Abstract--- Microalgae (MA)-derived products have garnered increasing interest, resulting in expanded large-scale farming. The substantial energy required for MA harvesting constitutes a significant obstacle. This study assessed the energy-efficient harvesting of MA using Ultra-Lower-Stress Membranes (ULSM) filtering (<20 kPa) in conjunction with oxygenation. ULSM provided numerous advantages, particularly in minimizing energy usage, as it functioned at low Transmembrane Stress (TMS). Elevated TMS frequently correlates with increased pumping power, augmenting energy consumption. Membrane (MM) compression would significantly impact MMs with elevated TMS. The findings indicated that MM compression leads to a pure water permeability (PM) loss of up to 65% when the TMS is increased from 2.4 to 20 kPa. The permeabilities of Chlorella vulgaris broth diminished from 1650 and 1200 to 280 and 260 $L/m^2 \cdot hr \cdot bar$ for the corresponding transmembrane pressures in systems with and without oxygenation. It was determined that MM fouled was more susceptible at low transmembrane pressure because inadequate foulant scoured from a low crossflow speed, resulting in PM reductions of up to 55%. MM fouling is the primary disadvantage of MM systems, as it diminishes MM efficiency. This research implemented aeration to prevent the fouling of MMs by dislodging foulants from the MM surface and holes. Reduced electrical consumption and improved filtering efficacy indicate that MM filtering integrated with an orifice presents a viable method for MA gathering, excelling in efficiency and accessibility. The particular electrical consumption for the ULSM was notably low, reaching up to 4.3 × 10^-3 kWh/m. A combination of low TMS and aeration results in minimal energy intake.

Keywords--- Microalgae, Filtering, Fouling Control, Harvesting, Energy-Efficiency.

Received: 18 - 10 - 2024; Revised: 26 - 11 - 2024; Accepted: 20 - 12 - 2024; Published: 30 - 01 - 2025

I. Introduction

Products derived from microalgae (MA), including food, feed, nutraceutical dietary supplements, beauty products, and biofuels, have garnered increasing interest, expanding large-scale microalgal biomass production (Abdelfattah et al., 2023). The extensive production of MA-derived goods has been constrained by the absence of an effective MA collecting method, primarily due to the diminutive size of MA cells, which have a culture density nearly equivalent to that of water. This minimal concentration necessitates the removal of substantial volumes of water, resulting in elevated energy consumption and processing expenses. Traditional MA gathering techniques, such as centrifugation, gravity settling, flotation screening, and flocculation, encounter significant restrictions (Anbarasu et al., 2024). These methods are either energy-intensive (centrifuging), time-consuming, or detrimental to algae biomass (biological coagulation), impeding their sustainable implementation.

The filtration process results in the accumulation of micro-sized algae cells on the Membrane (MM) flooring, resulting in fouling (Wang et al., 2023). Fouling causes a reduction in permeate flux by obstructing the MM pore sizes, either through individual cells and their byproducts or by forming a layer. It is crucial to alleviate the adverse yet natural occurrence from both operating and economic perspectives. A potent remedy to this issue is to induce shear stress on the MM terrain, disrupting the interactions between tiny algae cells and the MMs. Some instances of this strategy include elevated cross-flow speed, air scouring, and revolving disks. Its elevated efficiency is frequently undermined by the intricate device architecture and setup and the inevitable concern of preserving energy. Active filtration utilizing a spinning disk, albeit possessing exceptional effectiveness in

https://doi.org/10.67013/EPFS/V3I1/EPFS25105

filtration, is hindered by elevated device and operational costs (Ji et al., 2023). The principal objective of the shear-driven antifouling technique is to generate maximal shear strain on the MM area while minimizing energy usage.

MM-based filtering has come to be a viable alternative approach for the harvesting of MA. It employs minimal chemicals solely for infrequent cleaning, thereby preventing pollution of the final product; operates at ambient temperatures, which keeps certain active ingredients in the algae biomass (i.e., prevents protein decomposition); and, when implemented in an ongoing manner, facilitates the reuse of excess nutrients and culture mediums, thereby reducing spending and energy requirements. The benefits render MM-based algae biomass gathering appealing for processing various MA-derived products, encompassing low- and high-value items (Gautam et al., 2024).

The primary obstacle in MA gathering via MM processes is the fouling of the MM, which leads to a substantial decrease in flux and, more critically, increases energy use. The microscopic algae cells and their External Organic Material (EOM) can create a cake layer on the MM surface, which improves filtration difficulty over time, resulting in a loss of Permeability (PM) (Qiu et al., 2024). Cross-flow velocity, commonly utilized to dislodge foulants, facilitates the production of EOM, which exacerbates MM fouling.

This research necessitated effective fouling of MMs management that provides long-term efficiency with minimal energy input, achieved by implementing an Ultra-Lower Stress MMs (ULSM) filtration system in conjunction with aeration (air bubbling) (Zhao et al., 2022). ULSM is an appealing filtration technology since it provides minimal energy usage; yet, as an independent system without setup, it would be significantly impacted by MM corrosion. This results from inadequate force from ULSM to remove the foulant from the MM's area and gaps. Therefore, an MM fouling management mechanism must address this problem. This research employed air bubbling to mitigate MM fouling and enhance the efficacy of the ULSM filtering technology.

II. Background

Conditions for MA Cultivation

An aquatic microalga, was acquired from the Research Center of Bioengineering and Biotechnology. The tiny algae cells were cultivated with 1.2 g/L of s-feed (a commercialized media for cultivation) and 2.3% salinity in a 1-ton photobioreactor. The average weight of tiny algae cells was 0.8 g/L, with size variation ranging from 4 to 8 μm. Microalgal colonies were cultivated at a light concentration of 2400-3200 mol/m^2 and harvested during the static stage of development after six days of incubation. The algae cell density during the study period was 4.2 ± 0.5 × 10^7 cells/mL. Untreated cells were utilized immediately for the filtration test.

MM Filtering Utilizing an Orifice Plate

The efficacy of MM filtering was assessed utilizing a laboratory-scale cross-flow MM filtering apparatus, as seen in Fig. 1. An MM system was engineered to accommodate two flat MMs, allowing the porous supporting layer to orient towards the permeate surface. The ultrafiltration MMs, featuring a successful filtering surface of 25 cm^2 (2 cm in width and 9 cm in length), were installed in the MM modular. An aperture plate was created and mounted on the frontal section of the MM component to induce turbulence using thrust force from the feeding solution. The hollow plate was laser-perforated to produce varying quantities of holes, each having a diameter of 0.6 mm. Orifice apertures were included in the flow stream (2 cm length, 0.4 cm elevation). The penetrations were arranged horizontally and equally distributed inside the MM's intake region to ensure homogeneous turbulence creation across the MM intake. This investigation utilized 25, 15, and 9 holes. A substrate with a practical opening area of 0.5 cm^2, equivalent to the cross-flow input region, was used as a monitoring device for MM filtering. The overall intake surfaces of the orifices were 0.05 cm^2, 0.04 cm^2, and 0.02 cm^2 for 2, 15, and 9 holes, correspondingly. At an average feed rate of 3.5 L/min, with a Trans microalgae Stress (TMS) of 0.8 bar, the inlet pressures for each condition corresponded to 0.8 bar, 1.1 bar, 1.8 bar, and 4.7 bar (Peng et al., 2024). Using Bernoulli's equation, the thrust pace was determined as the highest achievable linear speed traveling through orifices. The elevated linear speed was anticipated to induce turbulence immediately following the orifice apertures impacting the MM face.

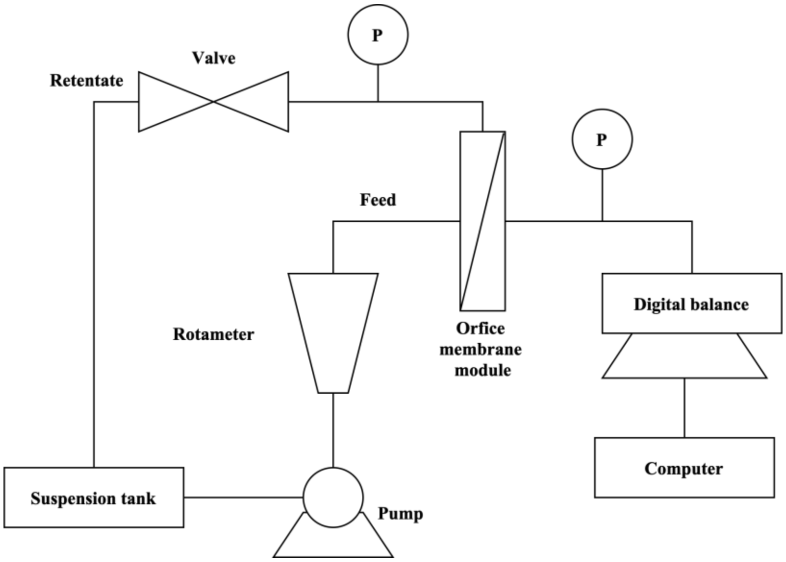

Figure 1: MM Filtering Device

Before collecting MA, an MM was compressed at TMS for a minimum of 35 minutes to stabilize the flux with deionized water and then reduced to 0.8 bar to guarantee homogeneous water PM. The mean pure water flux was 270.2 ± 15.5 L/m^2/h (LMH). After confirming water PM, 5 liters of MA dispersion was substituted for the actual filtration process. MA filtering was conducted for 65 minutes to evaluate the rate of fouled generation caused by the target foulant. Following filtering, the cake-like layer that developed on the outermost layer of the MM was removed using deionized water, and water conductivity was assessed to evaluate the extent of contamination. All studies were performed at 28°C to avert any deterioration of the MA solution caused by heat. The temperature was maintained at a consistent level by a cooling water supply. Every test was conducted in duplicate to reduce mistakes.

Estimation of Energy Use

A hypothetical component was designed to assess the energy usage of a full-scale filtering structure, utilizing operating data derived from the filtering experiments conducted. In the non-aerated structure, all energy consumption was solely ascribed to the energy required for feed pumps. Supplementary aeration energy was incorporated into the aerated system. The complete component was presumed to be oriented upward, with a successful screen width of 1.5 m and an overall height of 2.5 m. The interval between two contiguous panels, forming the conduit for the supply flow, was established at 3 × 10^-3 m. The crossover speed and TMS were identical to those utilized in the tests. The calculation incorporated the friction degradation along with the component. The output for feed pumps (FP_P,kW) and the feed pumped efficiency (FP_EkWh/m') for fluid flow filtering were calculated using Eqs. (1) and (2), accordingly.

$$FP_F = Q_p\left(\frac{\Delta P}{p_F} + \frac{(V_C)^2}{2} + F\right) \tag{1}$$

$$E_P = n_F\,\frac{P_F}{V} \tag{2}$$

Where Q represents the volumetric speed of the feed traversing the path of flow (m/s), P_F denotes the weight density of the feed (assuming to be 1,000 kg/m^3), ΔP signifies the TMS (FP_a), V_c indicates the mean flow speed in the flow channels (m/s), the friction factor is expressed in J/kg, n_P refers to the pump energy consumption (set at 80%). V represents the dimensional velocity of the permeates (m/h), which can be computed from the parameters of permeation, TMS, and the total MM space within the flow channels (2 positions x height x length of the screen).

The aeration energy (E_A, kWh/m^3) was calculated using a method outlined in a different source, as presented in Eq. (3). According to the hypothetical full-scale component, the flow channel size A_i, defined as the gap length, which measures 2.5 × 10^-3 m, situated between the two screens through which the feed liquid and air traverse. The air traverses the MM region of A = (2 sides breadth x height) = 5.0 along the flow stream. The bubble's cross-flow speed (U, m/s) was established to match what was utilized in the test. The air pressure reaches the fluid flow channel (P_A,P_a) 10% above the liquid tension. The filtration flux (J) was established based on the experimental results. Additional factors like temperature (T), blower effectiveness (v), the height of the aerator nozzles from the fluid surface (y), and the aerator constants (1) were considered to be 300 K, 85%, 2.5 m, and about 1.5, correspondingly. This strategy does not account for the total energy use. The entire particular energy usage (E_T, in kWh/m^2) was the aggregate of the specific flowing and aeration power, as illustrated in Eq. (4).

$$E_A = \frac{P_A T_v}{2.7*\alpha(V-1)} \frac{VA_i}{JA} \left(\frac{j+FP_A}{FP_A} - 1\right) \tag{3}$$

$$E_T = E_A + E_p \tag{4}$$

III. Results

Figure 2(a) and 2(b) illustrate the impact of pressure on the PM and flow of clean water. Both flow and PM demonstrate the imposed transmembrane pressure's significant effect on MM compaction. The notable reduction in PM at elevated TMS indicates the significance of MM compression. MM compression denotes the physical compaction of the MM resulting from the applied TMS. The PM diminishes markedly from 2880 L/m^{2}hr·bar at a TMS of 2.6 kPa to approximately 378 L/m^{2}hr·bar at a TMS of 19 kPa. This behavior is closely linked to the hydration condition of the MMs, as water is expelled when stress is elevated. The forces exerted on the structure of MMs lead to reduced PM due to MM compacting, primarily in pressure-driven MM usage. A reduction in penetration as an indicator of MP directly indicates MM compaction.

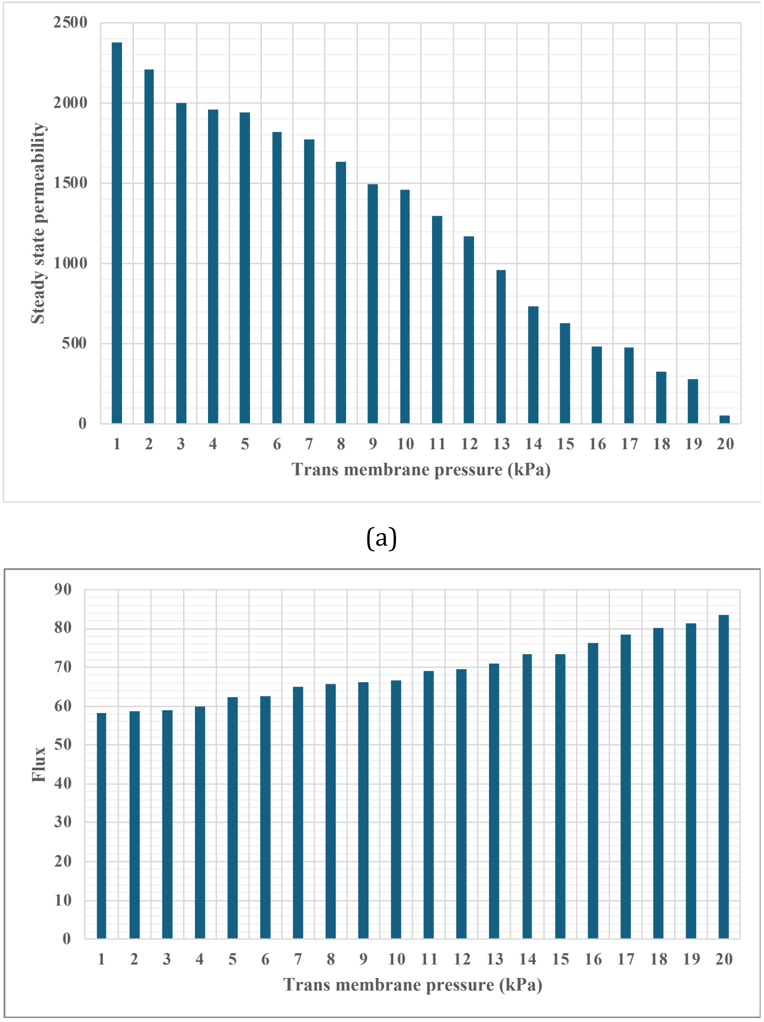

(a)

(b)

Figure 2: (a) PM and Fig. 2(b) Flux Analysis

Figure 3 illustrates that the permeation trend for Chlorella vulgaris broth filtering as a function of time spent in infiltration resembles that of pure water filtering. The reduction in porosity of clean water is due to MM compacting, whereas the decrease in porosity for chlorine-based broth filtration results from MM compression and fouling. The disparity between pure water and chlorine-contaminated broth can be attributed to the influence of fouling of the MMs under the assumption that compaction is exclusively influenced by the TMS and not by the feed. The water's pure PM was assessed at each testing level to distinguish the impact of the MM fouling from that of MM compacting. Fouling of the MM can be quantified as a variance in the porousness of clean water and that of the Chlorella vulgaris media.

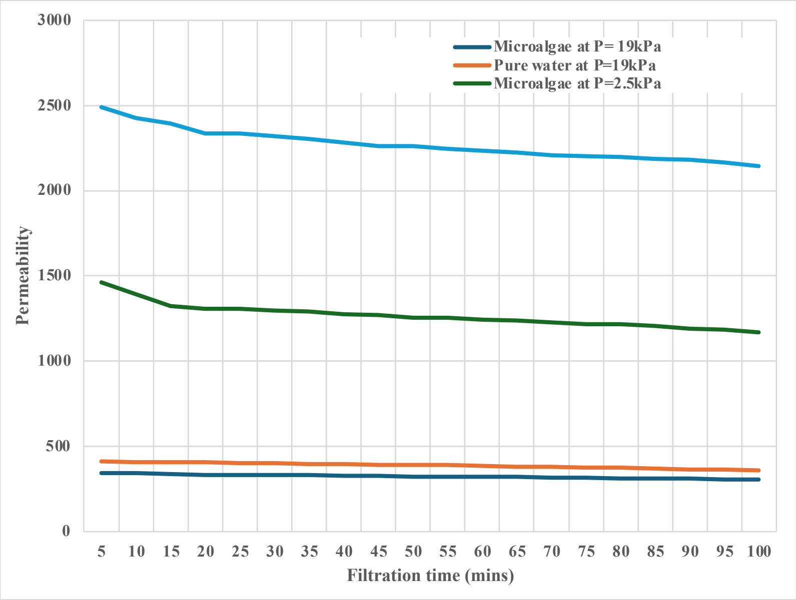

Figure 3: PM Analysis

Figure 4 (a) and 4(b) illustrate PM and flux as an indicator of TMS for two distinct systems: one without oxygenation and the other with oxygenation. The PM history for the two systems declined as TMS increased, whereas the flux trend increased with rising TMS for the two systems. The outcomes indicate the significance of TMS selection, as it serves as the basis for filtering. The MM is prone to significant fouling and reduced flux at low crossflow speed and TMS. At high TMS, the MM can increase flux by enhancing the driving force and decreasing fouling inclination, albeit at the cost of elevated mechanical pump power. Minimizing losses in mechanical power is essential to attain optimal MM filtering efficiency. Energy loss is typically associated with power, pumps, MMs, valves, and system architecture. Therefore, choosing the optimal TMS for the MM structure is essential for maximum effectiveness.

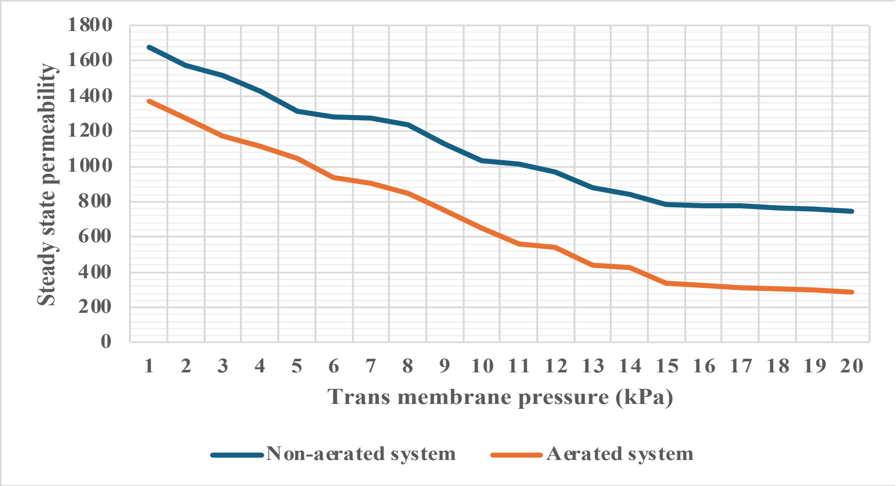

(a)

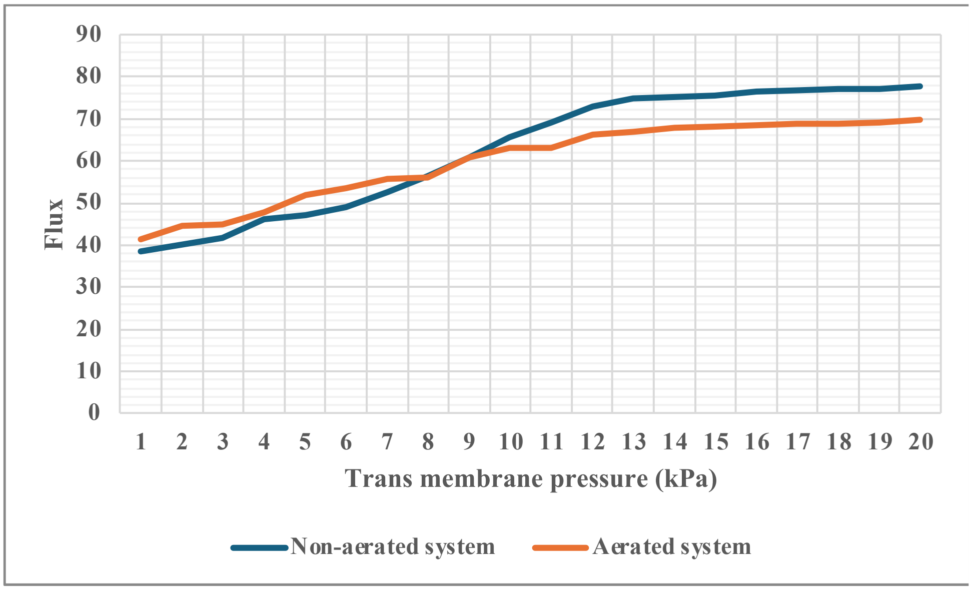

(b)

Figure 4: (a) PM and Fig. 4(b) Flux Analysis

Figure 5 illustrates that energy usage progressively escalates at elevated TMSs and aeration speeds for both systems with and without aeration. Energy use was assessed to identify optimal MM effectiveness with minimal energy usage, a crucial element in the MA harvesting procedure. The byproducts of MA constitute the primary expense in manufacturing MA-based goods, with 25-32% of the total manufacturing expenses attributed to the collecting phase. Both aerated and non-aerated systems exhibited an increase in energy usage at elevated TMS. The aerated network utilized more energy than the non-aerated structure, attributable to the supplementary energy required for the aeration implemented to mitigate MM fouling in the entire system. It is important to note that in the configuration employed in this work, the aeration rate escalated as the TMS, resulting in elevated aeration energy at greater TMS. In all instances, the non-aerated structure's power consumption is consistently lower than that of the aerated structure, indicating that the fouling management facilitated by aeration can be more energy-intensive than the crossflow speed generated by elevated TMS.

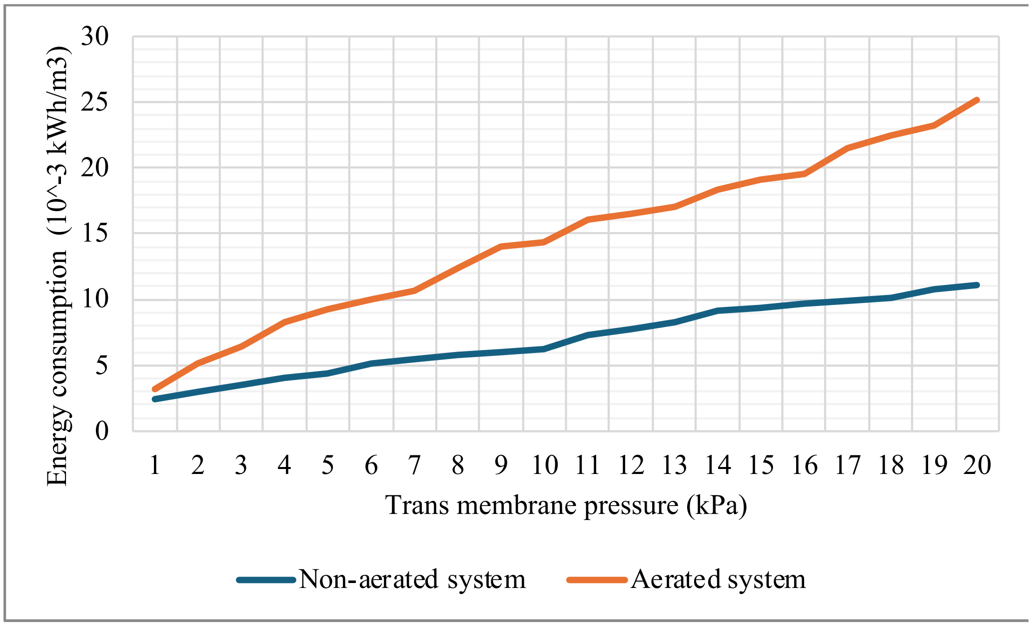

Figure 5: Energy Consumption Analysis

IV. Conclusion

Despite numerous strategies to mitigate fouling difficulties in MM filtration, no singularly effective anti-fouling method has emerged for widespread application. The present research illustrates the efficacy of ULSM in reducing energy input for filtering Chlorella vulgaris soup—elevated TMS significantly impacted MM compaction, resulting in a decrease in porosity. The PM of Chlorella vulgaris broth diminishes from 1650 and 1200 to 280 and 260 L/m^2·hr·bar as TMSs increase from 2.58 to 20 kPa. Reduced TMS diminishes compaction but increases susceptibility to MM fouling. Combining the effects of TMS and aeration, low TMS and agitation can yield a minimal energy consumption of up to 4.5 × 10^-3 kWh/m^3. This work presents a novel method for energy-efficient and fouling-resistant MM filtration in MA extraction. Aeration is a method to mitigate fouling on the MM's edges and holes by creating hydrodynamic conditions that generate drag and lift forces capable of dislodging foulants from the barrier. Aeration can enhance MM efficiency, while its installation will increase energy use. According to the power use assessment in this investigation, the energy usage of the aerated systems is considered minimal compared to the literature provided. All literature indicated that orifice-based turbulent creation is a robust anti-fouling method in MM filtering for algae harvesting, characterized by structural ease and significant application potential.

References

[1] Abdelfattah, A., Ali, S. S., Ramadan, H., El-Aswar, E. I., Eltawab, R., Ho, S. H., ... & Sun, J. (2023). Microalgae-based wastewater treatment: Mechanisms, challenges, recent advances, and future prospects. *Environmental science and ecotechnology*, *13*, 100205. https://doi.org/10.1016/j.ese.2022.100205

[2] Anbarasu, I., Palanivel, P., Saravanakumar, S., & Gangatharan, M. (2024). Collection and Processing of Microalgae from Coralloid Roots of Cycads. In *Plant Microbiome Engineering* (pp. 27-30). New York, NY: Springer US. https://doi.org/10.1007/978-1-0716-4180-4_4

[3] Wang, H., Hu, H., Chen, S., Schwarz, C., Yin, H., Hu, C., ... & Huang, J. (2023). UV pretreatment reduced biofouling of ultrafiltration and controlled opportunistic pathogens in secondary water supply systems. *Desalination*, *548*, 116282. https://doi.org/10.1016/j.desal.2022.116282

[4] Ji, X., Huang, J., Teng, L., Li, S., Li, X., Cai, W., ... & Lai, Y. (2023). Advances in particulate matter filtration: Materials, performance, and application. Green *Energy & Environment*, *8*(3), 673-697. https://doi.org/10.1016/j.gee.2022.03.012

[5] Gautam, R., Patial, S. K., & Singh, S. (2024). Algae Biomass: Importance, Harvesting Techniques, Extraction Methods, and Associated Challenges. In *Value Added Products From Bioalgae Based Biorefineries: Opportunities and Challenges* (pp. 67-94). Singapore: Springer Nature Singapore. https://doi.org/10.1007/978-981-97-1662-3_4

[6] Qiu, X., Wang, J., Xin, F., Wang, Y., Liu, Z., Wei, J., ... & Zheng, X. (2024). Compensatory growth of Microcystis aeruginosa after copper stress and the characteristics of algal extracellular organic matter (EOM). *Chemosphere*, *352*, 141422. https://doi.org/10.1016/j.chemosphere.2024.141422

[7] Zhao, Z., Blockx, J., Muylaert, K., Thielemans, W., Szymczyk, A., & Vankelecom, I. F. (2022). Exploiting flocculation and membrane filtration synergies for highly energy-efficient, high-yield microalgae harvesting. *Separation and Purification Technology*, *296*, 121386. https://doi.org/10.1016/j.seppur.2022.121386

[8] Peng, H., Fu, J., Huang, Y., Xia, A., Zhu, X., Zhu, X., & Liao, Q. (2024). Deciphering mechanism of sulfide stress on microalgae and overcoming its inhibition by regulation growth acclimatization period. *Chemical Engineering Journal*, *495*, 153045. https://doi.org/10.1016/j.cej.2024.153045